Journal of Structural Engineering & Applied Mechanics
2021 Volume 4 Issue 1 Pages 028-045
https://doi.org/10.31462/jseam.2021.01028045
www.goldenlightpublish.com

RESEARCH ARTICLE

Experimental, numerical and analytical investigation on blast response of brick walls subjected to TNT explosive

Ahmet Can Altunışık[1], Fatma Önalan[2], Fezayil Sunca[*3]

[1] *Karadeniz Technical University, Department of Civil Engineering, Trabzon, Turkey*
[2] *General Directorate of Water and Sewage, Ankara, Turkey*
[3] *Sivas Cumhuriyet University, Department of Civil Engineering, Sivas, Turkey*

Abstract

Structural damage caused by terrorist attacks or explosions resulting from accidents is an essential crucial issue for civil engineering structures. After the explosion, heavy damage and total collapse occur in the structural carrier system, and these destructions can cause significant loss of life and property. This study aimed to determine the structural behavior of brick walls exposed to blast loading with different explosive weights using analytical, numerical, and experimental methods. The masonry brick walls were selected for the application and constructed in the allowed quarry area for experimental studies. 40g, 150g, and 290g of TNT, which are placed inner base center of brick walls, were used respectively to observe the progressive damage. The analytical blast responses, such as maximum pressure values etc., were calculated and predicted empirical formulas. The numerical blast responses were determined with Ansys Workbench and Autodyn software. At the end of the study, damage situations, pressures, displacement values, and energies are presented comparatively. It is observed from both experimental and numerical methods that 40g and 150g TNT explosives caused several damages on the wall. The wall collapsed on supporting points in 290g TNT explosives. It can be seen that the mean values of pressures and displacements increase respectively by three and six times, with the TNT explosive weight increasing from 40g to 290g. A good agreement is also found between the finite element results and empirical formulas proposed by Henrych and Sadovsky. However, inconsistent blasting responses are obtained with empirical formulas depending on the scaled distance.

Keywords

Blast loading; Brick walls; Explosion; Explosive weights; Structural damage; TNT explosive

Received: 18 January 2021; Accepted: 24 February 2021
ISSN: 2630-5763 (online)

1. Introduction

The explosions caused by terrorist attacks and/or accidents have become an increasingly important issue for engineering in recent years. These explosions that may occur inside or near the structures cause structural severe damages or collapse severe economic losses and, more importantly, endanger public safety [1]. The explosion is a sudden, large-scale, high-speed, and high-energy generated by terrorist attacks or accidents. The loads resulting from these explosions affect the structures and the environment dynamically.

Masonry walls are critical structural components and widely used as structural and non-structural-elements in civil engineering structures.

* Corresponding author
Email: fsunca@cumhuriyet.edu.tr

The damages and/or failures of the walls subjected to explosive materials may lead to high-speed debris or structural collapse and may cause significant life and economic losses [2].

Many damages have occurred/observed in structural carrier systems due to explosions in the last twenty years. Mainly, meaningful life and economic losses occurred after the bomb attack on the Federal Murrah building in the USA in 1995; the bomb attack in Indonesia in 2002; the trinitrotoluene (TNT) attack on the Canal Hotel in Iraq in 2003; bomb attack on trains in Spain and India in 2004 and 2006; the explosions caused by the global gunpowder production facility and the terror attack in Turkey in 2008 and 2016. Fig. 1 shows some photographs from the explosions based structural damages

In the literature, many studies evaluate the explosion effect on structural behavior using empirical formulas and numerical methods. The first essential studies about blast response were carried out by Hopkinson and Cranz [4]. The studies have accelerated since the mid-center of the 20th century. The several empirical formulas based on the scaled distance to calculate the peak overpressure developed by researchers [5-10]. The scaled distance was calculated according to the explosion distance and explosive weight.

As well as empirical methods that are inadequate in many perspectives, advances in computer technology have enabled to use of analysis programs that can represent blast response more correctly. These developments motivated the researchers to obtain the blast responses of structures using finite element (FE) analysis based numerical methods. In the literature, effects of blasting on the structural behavior were handled for buildings [11-18], bridges [19-23], art structures [1,24], and historical structures [25]. It can be seen in the literature review that many studies have been performed to investigate blasting responses of various structures by using finite element models. Similarly, the blasting responses of masonry walls or infill walls have been numerically studied from various perspectives. Eamon et al [26] performed numerical blasting analyses of concrete masonry walls for different blast pressures and compared the numerical results with experimental data for the accuracy of finite element models. Wu et al [27] carried out the dynamic analyses of masonry structures and infill walls under blast-induced ground excitations. Wu and Hao [28] investigated the role of scaled distance on the damage level of masonry infilled RC structures exposed to airblast load and purposed minimum scaled distances for these structures. Wei and Stewart [29] used new models for strain rate effects and plastic damage of brick and mortar. Moreover, they performed the parametric studies on blasting response of brick walls using several parameters such as the boundary conditions, wall thickness, etc.

Moreover, experimental studies that are carried out to determine the blast responses of masonry walls are very limited..

Fig. 1. Some photographs from explosions based structural damages [3]

This is due to measurement costs, construction difficulties, risks, and long term official procedures. Davidson et al [30] experimentally investigated sprayed-on polymers' role to blasting resistance of unreinforced concrete masonry walls. Baylot et al [31] carried out experimental tests to determine the concrete masonry wall's hazard levels and researched the retrofitting methods to increase the blasting resistance of the walls. Zapata and Weggel [32] proposed the two criteria to evaluate the blast performance of a two-story unreinforced masonry structure. Chen et al [33], Alsayed et al [34] experimentally studied various retrofitting techniques to improve blasting performance of masonry infill walls. Keys and Clubley [35] suggested a method to estimate the debris distribution of masonry structures using numerical and experimental tests that were performed with nine structures. Li et al [2] and Gu et al [36] carried out experimental and numerical studies on blasting responses of masonry walls exposed to gas explosions.

The experimental studies carried out to determine the effects of explosions on the structures can not be generally preferred due to the construction's difficulty, measurement cost, risks, and formal procedures. In place of this, numerical and analytical studies are conducted in the literature. However, the blasting loads cause considerable complex effects on the structures. The analysis parameters selected for numerical models significantly affect structural behavior and results. Therefore, it is vital to choose the appropriate parameters for the reliability of the numerical analyzes. This paper aimed to determine the structural behavior of brick walls exposed to blast loading with different explosive weights using analytical, numerical, and experimental methods. For this purpose, the masonry brick walls having a brittle collapsing mechanism even at low-scale blasts were selected for the application and constructed in the allowed quarry area for experimental studies. Experimental studies were conducted by using 40g, 150g, and 290g of TNT, respectively, which were placed inner base center of brick walls, to evaluate the progressive damage. These charge weights were considered to investigate the blasting responses and behaviors of the wall in undamaged, damaged, and collapsed situations. Several empirical formulas were used to validate the experimental results, and finite element analyses were performed using Ansys Workbench and Autodyn software [37,38]. Fig. 2 shows the flowchart of the study.

2. Blast theory

2.1. Blast wave

The explosion that occurs by chemical reactions of solid, liquid, or gas explosives is described as a sudden release of energy with large-scale, high-speed, high-energy, high-density, and large-pressure [39]. The release of energy causes a very rapid chemical reaction during the explosion. The explosion is an exothermic reaction, which begins to spread like a shock wave in the materials and spread throughout the reaction.

Explosion waves occur with the burst of high-intensity explosives. As shown in Fig. 3, these waves produce a shock wave effect that spreads from the explosion center to the atmosphere in hemispherical form. From the moment the shock waves are released from the explosion center, it reaches a maximum pressure P_{so} and velocity in a short time such as a millisecond. As the shock wave moves away from the explosion center, the wave's surface area expands and the corresponding pressure value gradually decreases. This process continues until the equilibrium with the air surrounding the shock wave is achieved. This process is defined as the positive phase duration t_o .

During the propagation of the shock wave, the pressure value of the region behind the shock wave falls below the ambient pressure and creates a negative pressure P_{so}^- (creating a vacuum effect). The negative pressure formation process is called the negative phase duration (t_o^-). The time history graph of blast wave pressure is given in Fig. 4.

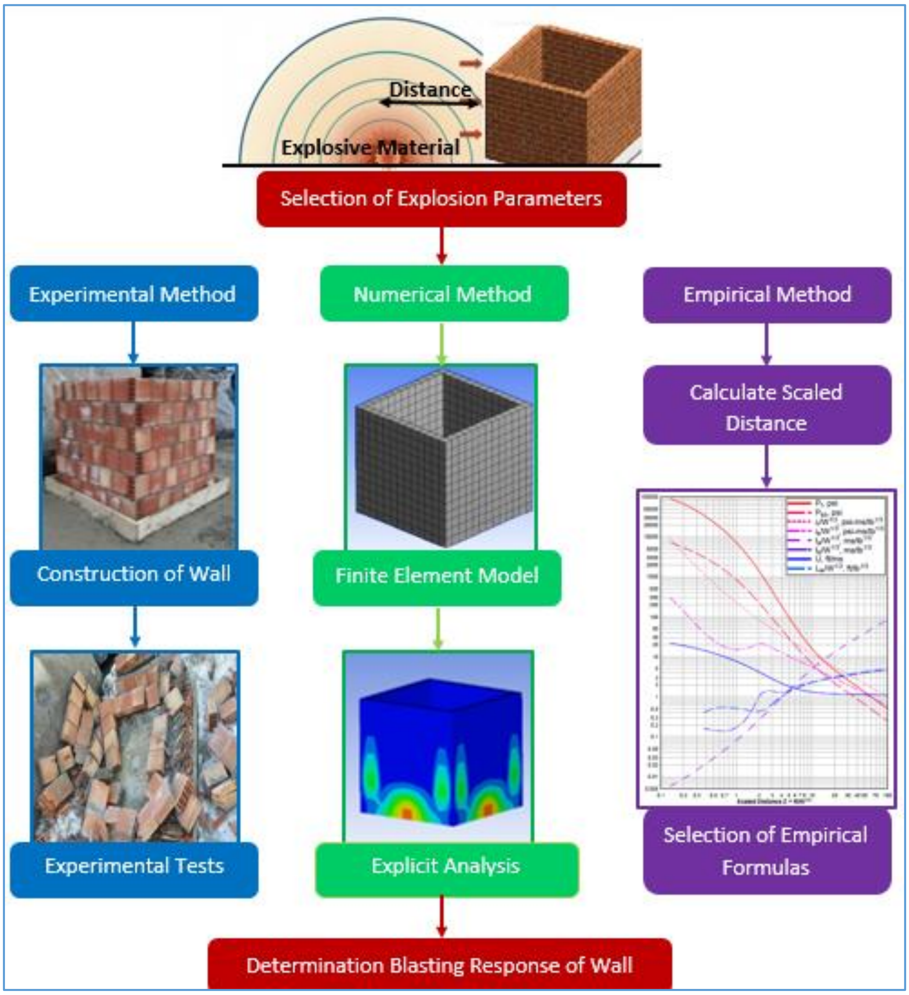

Fig. 2. The flowchart of the study

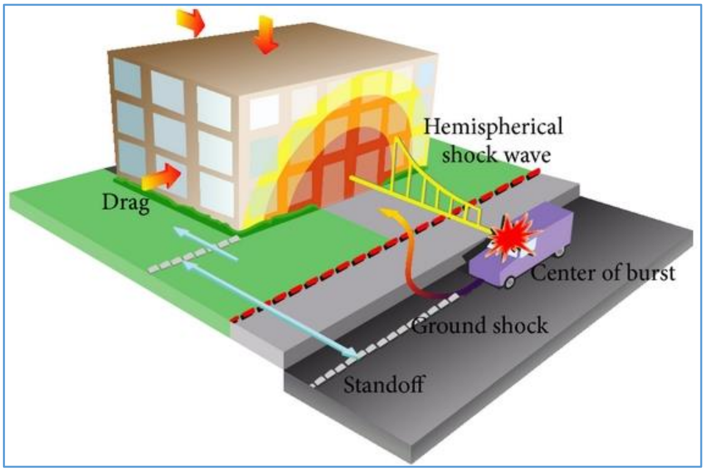

Fig. 3. Schematic representation of the propagation of blast loading [15,40]

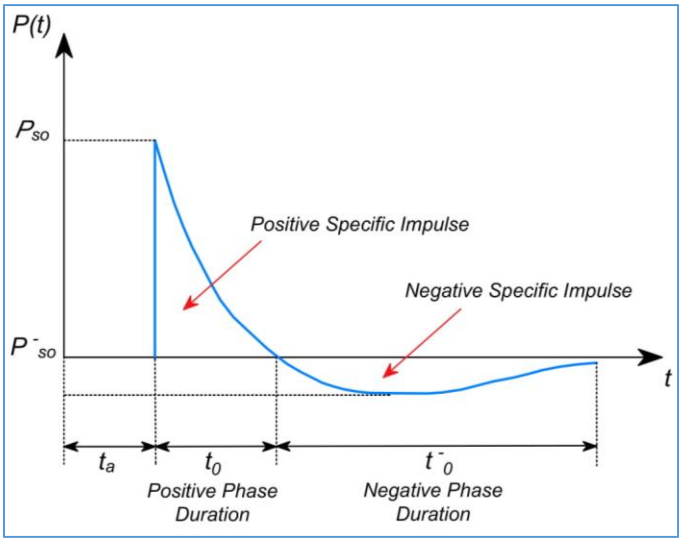

Fig. 4. Time history of blast wave pressure

2.2. *Empirical formulas*

Several empirical formulas were developed in the literature to calculating peak pressure caused by explosives. Generally, these formulas related to the scaled distance are calculated according to the explosive weight and distance between the explosion center and structure. In this study, peak pressure caused by explosives is calculated based on the methods purposed by Brode [5], Henrych [6], Kingery and Bulmash [7], Kinney and Graham [8], Mills [9], and Sadovskiy [10].

The scaled distance is represented by Z (mkg-1/3) and can be calculated by using Eq. (1). In Eq. (1), *R* and *W* are explosion distance (m) and explosives weight (kg), respectively.

$$Z = \frac{R}{\sqrt[3]{W}} \tag{1}$$

The formulas proposed by Brode in 1955 for calculating peak pressure based on the scaled distance are presented with Eq. (2).

$$\begin{aligned} P_{so} &= \frac{6.7}{Z^3} + 1 \quad P_{so} > 10 \text{ bar} \\ P_{so} &= \frac{0.975}{Z} + \frac{1.455}{Z^2} \\ &+ \frac{5.85}{Z^3} - 0.019 \quad 0.1 \text{ bar} < P_{so} < 10 \text{ bar} \end{aligned} \tag{2}$$

The formulas proposed by Henrych in 1979 for calculation of peak pressure based on the scaled distance are presented with Eq. (3).

$$\begin{aligned} P_{so} &= \frac{14.072}{Z} + \frac{5.54}{Z^2} - \frac{0.375}{Z^3} + \frac{0.00625}{Z^4} \quad 0.05 < Z < 0.3 \\ P_{so} &= -\frac{6.194}{Z} - \frac{0.326}{Z^2} + \frac{2.132}{Z^3} \quad 0.3 \le Z \le 1 \\ P_{so} &= \frac{0.662}{Z} + \frac{4.05}{Z^2} + \frac{3.288}{Z^3} \quad 1 \le Z \le 10 \end{aligned} \tag{3}$$

Kingery and Bulmash [7] proposed a polynomial formulation to calculate positive peak pressure and impulse. This formulation and constants are given in Eq. (4) and Table 1.

$$\begin{aligned} \Delta P_f &= \text{Exp}\Big[A + B\ln Z + C(\ln Z)^2 \\ &+ D(\ln Z)^3 + E(\ln Z)^4\Big] \end{aligned} \tag{4}$$

Kinney and Graham [8] proposed the empirical formula for peak overpressure based on scaled distance and ambient pressure as follows.

$$P_{so} = P_o \frac{808\left[1 + \left(\frac{Z}{4.5}\right)^2\right]}{\left\{\left[1 + \left(\frac{Z}{0.048}\right)^2\right]\left[1 + \left(\frac{Z}{0.32}\right)^2\right]\left[1 + \left(\frac{Z}{1.35}\right)^2\right]\right\}^{1/2}} \tag{5}$$

Table 1. The constants in Eq. (4)

Z (m/kg$^{1/3}$)	A	B	C	D	E
0.2-2.9	7.1206	-2.1069	-0.3229	0.1117	0.0685
2.9-23.8	7.5938	-3.0523	0.40977	0.0261	-0.01267
23.8-198.5	6.0536	-1.4066	0	0	0

The formulas proposed by Mills [9] and Sadovskiy [10] for calculation of peak pressures are presented with Eqs (6) and (7), respectively.

$$P_{so} = \frac{1772}{Z^3} - \frac{114}{Z^2} + \frac{108}{Z}\ \text{(kPa)} \tag{6}$$

$$\Delta P_f = \frac{0.085}{Z} + \frac{0.3}{Z^2} + \frac{0.8}{Z^3}\ \text{(MPa)} \tag{7}$$

Also, peak pressure values were calculated according to the graph given in "Structures to Resist the Effects of Accidental Explosions" [4]. In this graph, parameters such as peak pressure reflected pressure, impulse and velocity can be obtained depending on the scaled distance.

3. Description of brick walls

Within the study's scope, masonry walls were constructed by using brick elements with dimensions of 190mm×190mm×135mm and mortar with a thickness of 10mm. The hollow ratio was selected as 45% for brick elements by the requirements of the Turkish Building Earthquake Code [41]. The width, length, and thickness of each wall were considered 122cm, 113cm, and 8.5cm. There was no slab, and the wall's upper surface was built entirely open to the atmosphere. The walls were embedded in the foundation to represent the fixed boundary condition. The blasting loads have complex effects on the structures. Suppose the slab and different boundary conditions are considered during the experiments. In that case, various details such as the behavior of slab to wall connection and soil-structure interaction should be taken into account in the numerical analyses. This situation can cause the blasting effects on the wall to be more complicated. For this reason, the complexity of structural behavior was reduced with these conditions that were considered during the experiments.

The mechanical properties of the brick wall are given in Table 2. Many researchers recommend several values for the mechanical properties of brick walls. In this study, the mechanical properties are selected according to the requirements of TBEC. Fig. 5 shows the general views and drawings for masonry walls, also some photographs after construction are presented in Fig. 6.

4. Blast response of the masonry walls

4.1. Experimental method

Blast tests were conducted 28 days after wall construction for the mortar to reach 100% of its strength. The capsule-sensitive TNT explosives were placed inner base center of the brick walls. The test was firstly carried out with 40g TNT explosive, which caused micro-cracks on the walls. Then, the tests were repeated with 150g and 290g TNT explosives to gradually increase the cracks and collapse the walls. To prevent the explosive from scattering around due to the high-pressure, the TNT explosives were covered with a sand layer. Fig. 7 shows the capsule sensitive TNT and experimental test setup.

In blast tests carried out with 40g and 150g TNT explosives, it was determined that micro-cracks occur on the walls and the increase in the amount of explosives leads to the cracks to develop. Moreover, as a result of the blast test that is performed with 290g TNT explosive, it was observed that the wall collapsed by separating from the fixed supports. During the explosion, it was seen that brick fragments spread to the environment at high speed with high pressure. This situation shows that if the necessary security measures are not taken during the blast tests, serious dangers may occur for life and property safety. After blasting test conducted with 290g TNT explosive, some collapsed brick wall photographs are given in Fig. 8.

Table 2. Mechanical properties of the selected brick wall

Material	Modulus of Elasticity (kPa)	Density (g/cm^3)	Compressive safety strength (kPa)
Brick	2.88×10^6	0.70	800

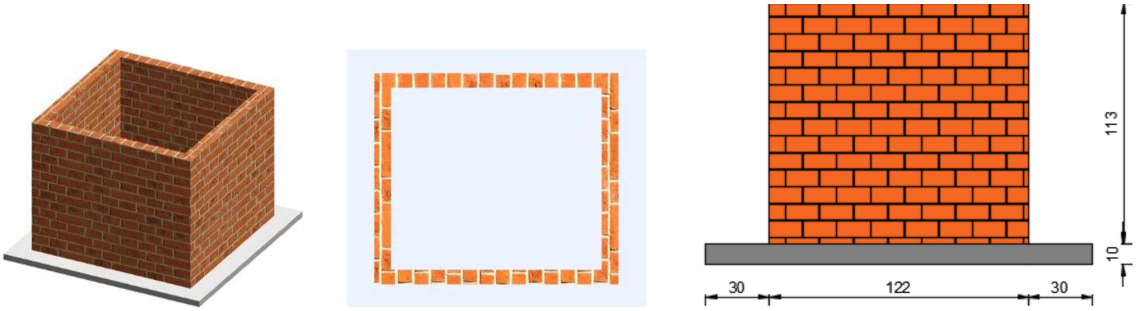

(a) Three dimensional view (b) Plan view (c) Two dimensional view and dimensions (all dimensions are in cm)

Fig. 5. General views and drawings for masonry walls with dimensions

Fig. 6. Some photographs of masonry walls after construction

Fig. 7. Capsule sensitive TNT and experimental test setup

Fig. 8. Some views from the collapsed masonry walls

4.2. Numerical analyses

Three dimensional FE model of the walls was firstly constituted using ANSYS Workbench software. The walls supports are considered as the fixed boundary condition. The Lagrange theory including calculations for the conservation of mass, energy, and momentum was used for solid elements. Three modeling approaches can be used in the FE model of masonry walls exposed to blasting loads: micro-modeling, simplified micro-modeling, macro-modeling. In this study, the macro-modeling approach was preferred. The mesh convergence study of the wall model was carried out using different mesh sizes for both solid elements and air volume. Modal characteristics such as natural frequencies and mode shapes were used as comparison parameters of mesh convergence study. The mesh size was chosen as 100mm for solid elements. To perform the explicit analyses, the FE model of the walls was transferred into Ansys Autodyn software.

For blast analyses, the air volume, in which the wall is placed, and TNT explosives are modeled according to Euler's theory. The mesh sizes were selected as 15mm for air volume and TNT explosives. In the Lagrange and Euler models, the fully coupled method was used to perform the explicit analyses, correctly. Fig. 9 shows the three dimensional FE model of the walls and TNT explosive placement.

The selection of correct material properties and material models is one of the most critical steps to obtain reliable results under high pressure in the nonlinear analysis. Otherwise, sudden changes within milliseconds cannot be monitored. For this purpose, the Riedel-Hiermaier-Thoma (RHT) model [42] and P-alpha [43] equation of state were chosen for brick elements. The air volume, which was contained the wall and explosives, was considered as the ideal gas. The Jones-Wilkens-Lee (JWL) equation of state, which reflects the rapid expansion and diffusion properties, was used for TNT explosives. In the blast analyses, 40g, 150g, and 290g of the capsule sensitive TNT explosive are modeled at the brick walls' inner base center. Table 3 summarized the selected models and material properties.

A total of 16 gauge points were selected on the walls to monitor the damage contour diagrams, pressures, and displacements. The selected gauge points are given in Fig. 10. The analysis duration and time increments were taken into account as 3 and 0.01ms, respectively, to observe the differences in pressure change more accurately.

To monitor the explosion substance effects on blasting responses of the walls, the time-histories of pressures at the different elevations are presented in Fig. 11. The pressure contour diagrams in the time step when the peak pressure is obtained are given in Fig. 12. It is shown from Figs. 11-12 that the peak pressures are found at the gauge 16 for all blasting scenarios. The gauge 16 is located in support of the wall and is closest to the explosion center. Also, many gauge points are examined to compare the peak pressures at the wall's different elevations. It can be seen from Fig. 11 that the maximum pressures are obtained as 0.34MPa at 0.50ms for 40g TNT explosive, 0.86MPa at 0.41ms for 150g TNT explosive, and 1.59MPa at 0.37ms for 290g TNT explosive.

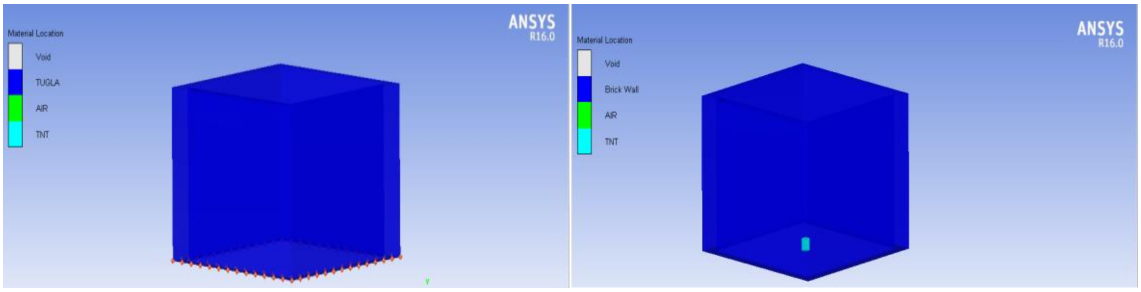

(a) Support conditions (b) TNT placement

Fig. 9. The three dimensional FE model of the walls and TNT explosive placement

Table 3. The selected models and material properties for brick, air volume and TNT explosives

Parameter/Material	Unit	Brick	Air volume	TNT
Equation State		P-alpha	Ideal gas	JWL
Strength Model		RHT	-	-
Density	g/cm^3	0.70	1.25×10^{-3}	1.63
Elasticity Modulus	MPa	2.88×10^3	-	-
Shear Modulus	MPa	1.19×10^3	-	-
Ambient Temperature	K	-	288.20	-
Specific Temperature	J/kgK	-	717.59	-
Threshold Energy	kJ/kg	-	2.07×10^5	3681.00
Detonation Velocity	m/s	-	-	6930.00
Unit Volume Energy	kJ/m^3	-	-	6.00×10^6
Pressure Value	MPa	-	-	2.00×10^4

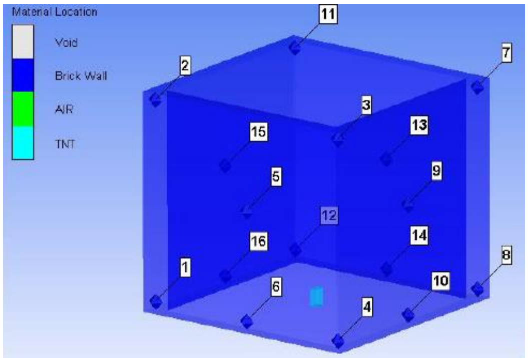

Fig. 10. The selected gauge points on the brick walls

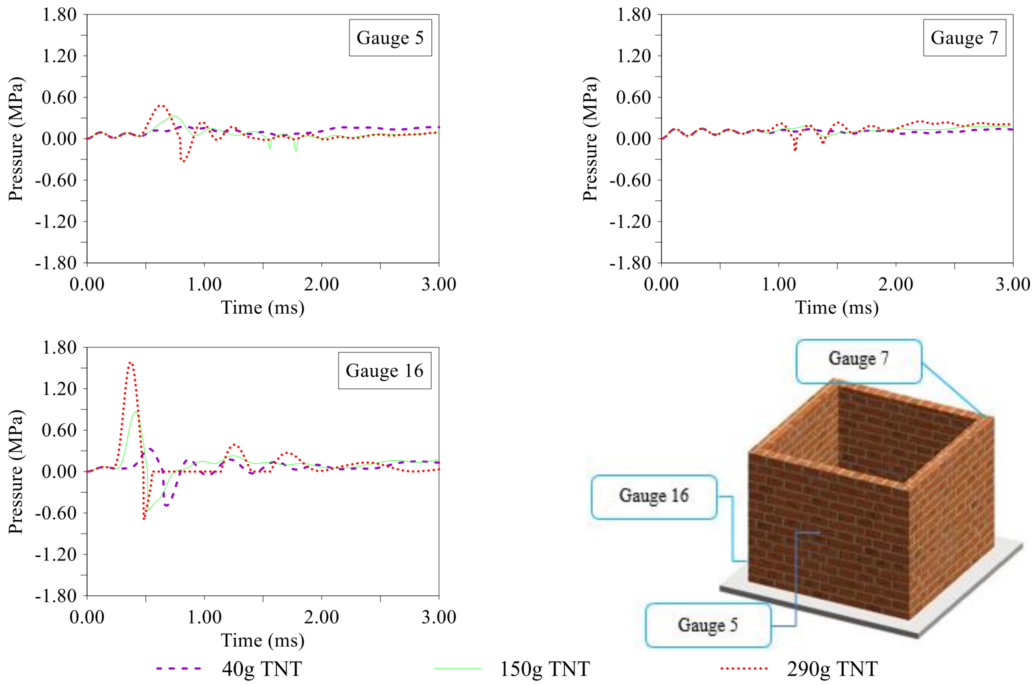

Fig. 11. The time-histories of pressures obtained from critical gauges of wall

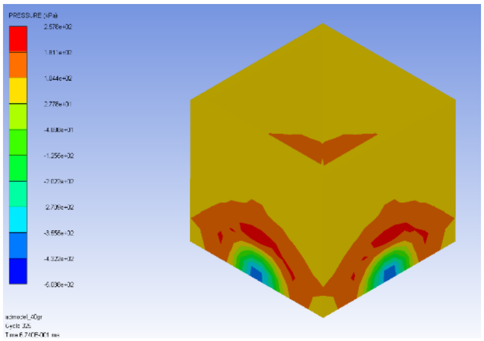

(a) 40g TNT explosive

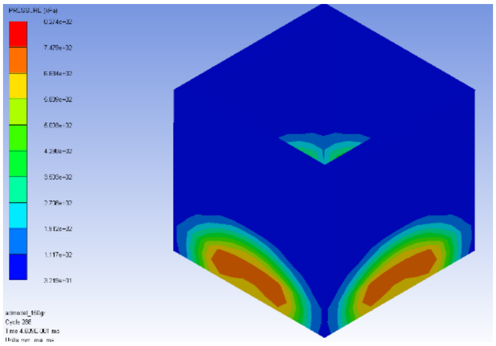

(b) 150g TNT explosive

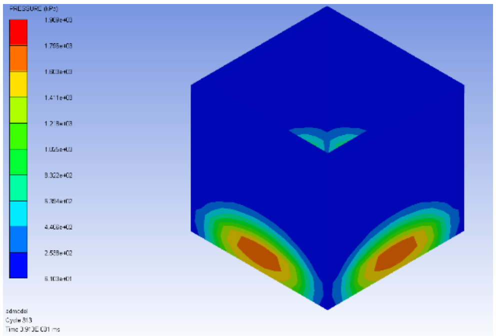

(c) 290g TNT explosive

Fig. 12. Pressure contour diagrams for different explosive weights

With the increase of charge weight from 40g to 290g, the peak pressure increase approximately 4.67 times. The pressure value of 1.59MPa for 290g TNT explosive is considerably greater than the allowable stress for brick elements. Also, the peak pressures obtained from the selected gauges gradually decrease along with the wall height. The results are compatible with the arrival times of the blast waves or the scaled distances, as observed in previous studies [33,35,45]. On the other hand, it is seen that the peak pressures occur in different time steps at each selected gauges. Although these differences are obvious due to the axis range of the graphs, the arrival time of peak pressures is less than 1ms along with the wall height. As a result, it can be said that different peak pressure values almost simultaneously arrive at all points of the wall. For the masonry wall, this situation has been emphasized by Chen et al [33] utilizing blasting test results.

The total released energy from the explosion, absorbed total energy by the materials and air volume are given in Fig. 15. It can be seen from Fig. 15; the released energies are obtained as $1.63\times10^{11}\mu J$ for 40g TNT explosive, $5.51\times10^{11}\mu J$ for 150g TNT explosive, and $11.01\times10^{11}\mu J$ for 290g TNT explosive, respectively. The air volume absorbs a significant part of the released energy for each charge weight. The total released energy has been absorbed by the air and other elements for 40g TNT explosive. However, the total energies caused by 150g and especially 290g TNT explosive have been not absorbed (Fig. 15). Therefore, many elements are damaged. The energy absorbed by the brick element is too small and can be neglected.

To monitor the explosion substance effects on damages, the time-histories of damage ratios at the critical region of the wall are presented in Fig. 16. The damage contour diagrams in the time step when the peak pressure is obtained are given in Fig. 17. It can be seen from Figs. 16-17 that the gauge 16 is critical in terms of damage ratios. The gauge 16 is located in support of the wall and is closest to the explosion center.

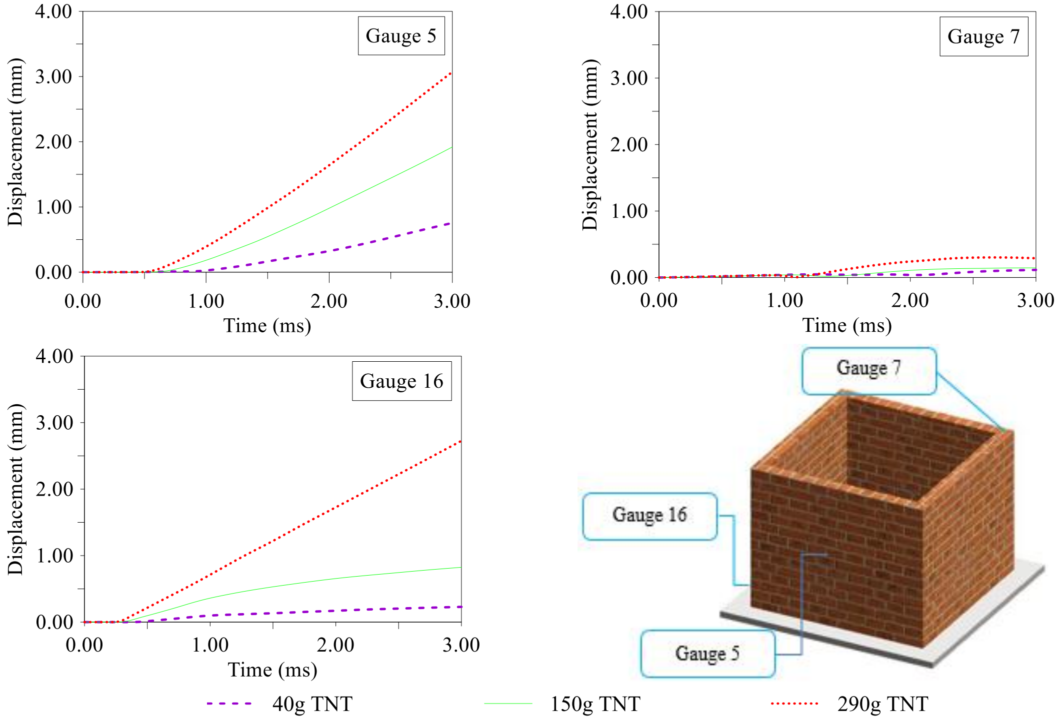

Fig. 13. The time-histories of displacements obtained from critical gauges of wall

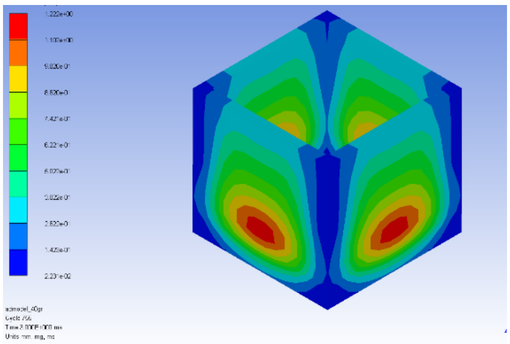

(a) 40g TNT explosive

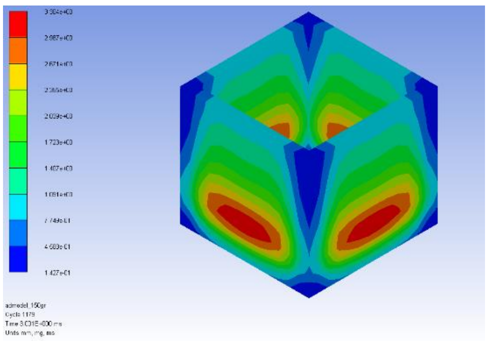

(b) 150g TNT explosive

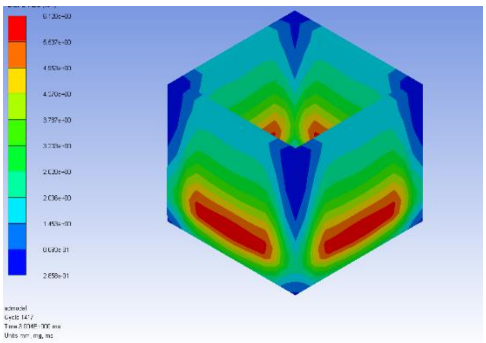

(c) 290g TNT explosive

Fig. 14. Displacement contour diagrams for different explosive weights

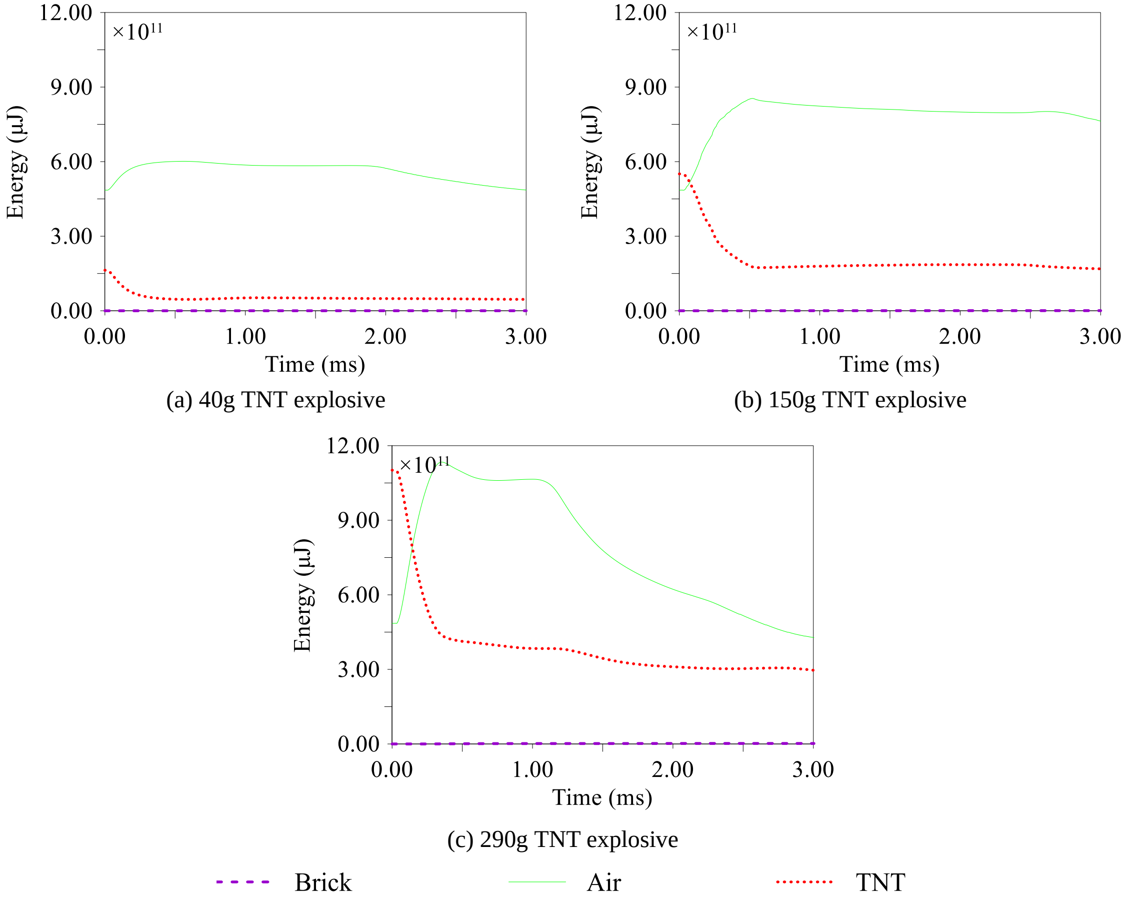

Fig. 15. The released energy from the explosion, absorbed energy by the materials and air volume

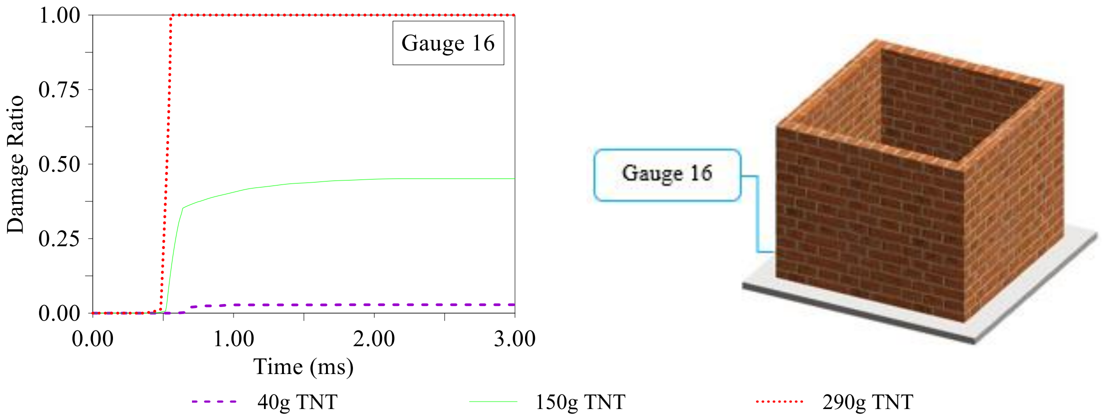

Fig. 16. The time-histories of damage ratios obtained from critical gauge of wall

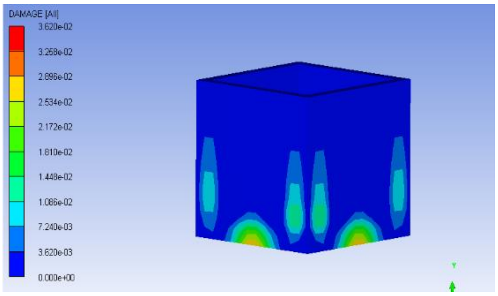

(a) 40g TNT explosive

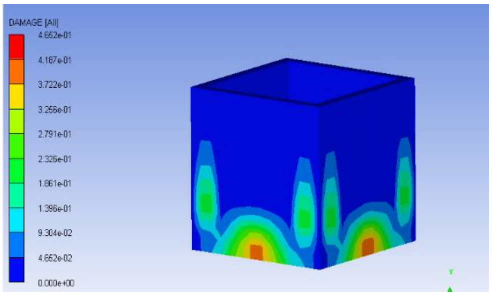

(b) 150g TNT explosive

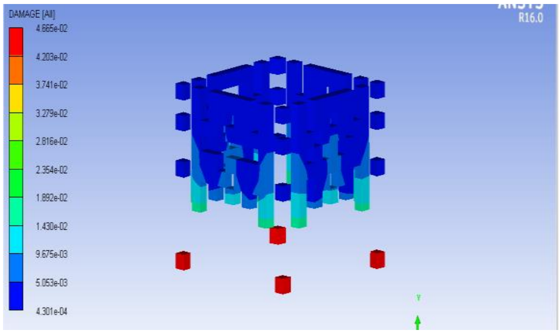

(c) 290g TNT explosive

Fig. 17. Damage contour diagrams for different explosive weights

Also, all gauge points are examined to compare the damage ratios at the wall's different elevations. The damage ratio takes values between 0 and 1. The fact that this ratio is close to 1 indicates the damage is intense. The damage ratios at gauge 16 are calculated as 0.03 for 40g TNT explosive, 0.45 for 150g TNT explosive, and 1.00 for 290g TNT explosive. As a result of the numerical analysis, it is determined that the damage ratios are significantly increased with the increase of charge weight from 40g to 290g. Moreover, it can be observed from Fig. 17 that similar to experimental tests; the wall collapsed by separating from fixed supports with 290g TNT explosive.

Chen et al [47] classified the damage levels based on the scaled distance to describe the damage levels of confined masonry walls under blast loads. For different damage situations, the scaled distance ranges defined to be more than 3m/kg$^{1/3}$ for low damage, 2m/kg$^{1/3}$ - 3m/kg$^{1/3}$ for medium damage, 1.6m/kg$^{1/3}$ - 2m/kg$^{1/3}$ for high damage, and less than 1.6m/kg$^{1/3}$ for collapse. In this study, blast tests were carried out with 40g, 150g, and 290g TNT explosives. It was determined that micro-cracks occur on the walls for 40g TNT and the increase in the amount of explosives from 40g to 150g caused the cracks to develop. Moreover, the wall collapsed under 290g TNT. The scaled distances of the gauge 16, which is the critical point in terms of blast responses of the wall, are 2.04m/kg$^{1/3}$ for 40g TNT, 1.31m/kg$^{1/3}$ for 150g TNT, and 1.05m/kg$^{1/3}$ for 290g TNT explosives. By comparing to scaled distances of the gauge 16 and damage ratios, it can be seen that the damage levels proposed by Chen et al [47] for confined masonry walls are partially conservative for the selected masonry wall. This is an expected situation due to various reasons such as wall units/mortar properties, boundary conditions, and experimental setup chosen in this study.

Only 4 gauge points are selected to evaluate the peak pressures considering symmetry in the lateral direction. These gauge points are 1, 2, 5, and 6. Table 4 summarizes the peak pressure values calculated according to the 40g, 150g, and 290g TNT explosives. Also, the differences in peak pressures were calculated based on FE results (Table 5).

Table 4. Peak pressure values for selected gauge points (MPa)

Gauge Point	Amount of TNT (g)	Z (m/kg$^{1/3}$)	Autodyn	Brode	Henrych	Kingery-Bulmash	Kinney-Graham	Mills	Sadovskiy	UFC 3-340-2
1	40	2.84	0.22	0.08	0.09	0.13	0.09	0.10	0.10	0.18
	150	1.86	0.45	0.18	0.20	0.33	0.25	0.30	0.26	0.35
	290	1.34	0.55	0.39	0.41	0.64	0.52	0.74	0.55	0.60
2	40	3.62	0.14	0.05	0.06	0.08	0.05	0.06	0.06	0.07
	150	2.39	0.19	0.11	0.12	0.17	0.14	0.16	0.15	0.19
	290	1.81	0.26	0.19	0.21	0.32	0.26	0.32	0.27	0.30
5	40	2.47	0.18	0.10	0.11	0.16	0.15	0.14	0.14	0.19
	150	1.62	0.33	0.25	0.27	0.42	0.34	0.44	0.35	0.40
	290	1.28	0.48	0.44	0.46	0.80	0.58	0.86	0.63	0.45
6	40	2.04	0.34	0.15	0.17	0.24	0.20	0.23	0.21	0.27
	150	1.31	0.87	0.41	0.43	0.74	0.55	0.79	0.59	0.80
	290	1.05	1.59	0.73	0.72	1.12	0.91	1.53	1.05	1.50

Table 5. The differences between the peak pressure values obtained from numerical methods and empirical formulas (%)

Gauge Point	Amount of TNT (g)	Brode	Henrych	Kingery-Bulmash	Kinney-Graham	Mills	Sadovskiy	UFC 3-340-2
1	40	65.84	60.50	41.61	58.22	54.52	54.52	18.88
	150	59.34	54.83	27.42	45.42	33.45	43.05	22.14
	290	29.82	26.77	-15.91	6.46	-33.48	0.01	-8.34
2	40	66.41	61.08	45.41	61.87	59.47	56.16	51.32
	150	42.31	33.86	6.75	25.84	16.42	20.92	-2.43
	290	24.85	16.85	-25.80	-1.10	-24.49	-5.33	-16.60
5	40	44.06	35.82	10.34	14.29	20.68	23.75	-6.54
	150	24.03	17.58	-27.61	-2.72	-32.84	-7.28	-21.70
	290	8.30	5.54	-65.56	-21.09	-78.37	-30.71	6.64
6	40	56.49	51.02	29.77	29.77	32.05	39.59	20.97
	150	52.48	50.68	14.60	36.91	8.67	32.23	7.75
	290	54.11	54.99	29.73	42.85	3.54	34.20	5.70

It can be seen from Table 4-5 that the differences between the peak pressure values obtained from numerical methods and empirical formulas decrease with the decreasing of scaled distance. For 40g TNT explosive, the maximum differences between FE analyses and empirical formulas are 66.41% for Brode, 61.08% for Henrych, 41.61% for Kingery-Bulmash, 61.87% for Kinney-Graham, 59.47% for Mills, 54.52% for Sadovskiy and 51.32% for UFC 3-340-2. For 150g and 290g TNT explosives, the maximum differences between FE analyses and empirical formulas are calculated as 59.54% with Brode and 78.37% with Mills.

5. Conclusion

In the design and analysis of civil engineering structures, various static and dynamic loads (dead, live, snow, wind, earthquake, etc.), which have shallow effects on structures than blasting loads, are widely used. This approach is required for economical designs. Because the rate of occurrence of blasting effects for any structure is meager. However, it was determined that even low charge weight can cause severe damage to walls due to this study. The extreme loads caused by explosions should be taken into account in the design and analysis of structures containing explosive substances and settlements close to gas stations. Its purpose is to prevent severe damage and/or collapse in structures, economic losses, and most importantly to protect public safety. The blasting loads cause considerable complex effects on the structures. Experimental methods can accurately define these complex effects. The experimental studies cannot be generally preferred due to several difficulties. In place of this, numerical and analytical studies are widely preferred in the literature. In numerical studies, the main problem is determining the appropriate analysis parameters such as equation states and strength models because the selected analysis parameters significantly affect structural behavior and results.

This study aimed to obtain the numerical models of brick walls by analysis parameters tuned with experimental results and to specify the structural behavior of brick walls exposed to blast loading with different explosive weights using analytical, numerical, and experimental methods. 40g, 150g, and 290g of TNT, which are placed inner base center of brick walls, were used respectively to observe the progressive damage. These explosive substances were considered to investigate the blasting responses and behaviors of the wall in undamaged, damaged, and collapsed situations. The masonry brick walls were selected for the application and built in the allowed quarry area for experimental studies. The analytical responses were predicted with empirical formulas. The numerical responses were determined with Ansys Workbench and Autodyn software. As a result of the experimental, numerical, and analytical studies, it was determined that the complex blasting effects could be accurately reflected by numerical models using the appropriate design parameters. At the end of the study, the following conclusions can be listed as:

<u>Experimental Method</u>

- In the experimental tests carried out for different blasting scenarios and explosive weights, it is determined that 40g and 150g TNT explosives led to several damages on the walls, and the walls collapsed by separating from the fixed supports with 290g TNT explosive.

<u>Numerical Analyses</u>

- It can be seen from the FE analyses that the maximum pressure values are obtained as 0.34MPa for 40g TNT explosive, 0.86MPa for 150g TNT explosive, and 1.59MPa for 290g TNT explosive.
- The maximum pressure value caused 290g TNT explosive is considerably significant than the brick element's allowable stress, and the walls collapsed with 290g TNT explosive similar to experimental tests.
- The maximum displacement values are calculated as 0.76mm for 40g TNT explosive, 1.92mm for 150g TNT explosive, and 3.08mm for 290g TNT explosive. With the increasing charge weight from 40g to 290g, the maximum displacement increases approximately 4.05 times.
- The total released energy has been absorbed by the air and other elements for 40g TNT explosive. However, the total energies caused by 150g and especially 290g TNT explosive have not been absorbed. Therefore, many damages occur on the wall.
- The energy absorbed by the brick element is too small and can be neglected.

- The damage ratios are calculated as 0.03 for 40g TNT explosive, 0.45 for 150g TNT explosive, and 1.00 for 290g TNT explosive. The damage ratios are significantly increased with the increase of charge weight from 40g to 290g.

Empirical Formulas

- Depending on the decreases in the scaled distance, the peak pressure values obtained from FE analyses and empirical formulas become more consistent.
- For 40g, 150g, and 290g TNT explosives, the maximum differences between FE analyses and empirical formulas are 66.41% with Brode, 59.54% with Brode, and 78.37% with Mills, respectively.
- The peak pressure values that are obtained from empirical formulas proposed by Kinney and Graham [8], Sadovsky [10], and UFC3-340-02 [44] are closer to FE analysis results depending on the decrease in scaled distance.

Because the number of the conducted case studies is quite limited, the meaningful curves and efficient conclusion to understand the behavior of one type of brick wall structures to TNT explosive are not presented to benefit the design of this type of structure. Therefore, the number of experimental studies should be increased within the scope of future studies. Considering the analysis parameters specified and experimentally checked as a result of this study, it will be possible to obtain the structural behavior of many engineering structures more efficiently and accurately by numerically besides analytical formulas.

Declaration of conflicting interests

The author(s) declared no potential conflicts of interest with respect to the research, authorship, and/or publication of this article.

References

[1] Toy AT, Sevim B (2017) Numerically and empirically determination of blasting response of a RC retaining wall under TNT explosive. Advances in concrete construction 5(5):493-512.

[2] Li Z, Chen L, Fang Q, Hao H, Zhang Y, Xiang H, Chen W, Yang S, Bao Q (2017) Experimental and numerical study of unreinforced clay brick masonry walls subjected to vented gas explosions. International Journal of Impact Engineering 104:107-126.

[3] URL-1, http://www.haberlerim.com.tr/gundem/2016-yilinda-turkiyede-yasanan-bombali-saldirilar-h9176.html.

[4] Hopkinson B, Cranz C. Cube Root Scaling Law. 1915.

[5] Brode HL (1955) Numerical solutions of spherical blast waves. Journal of Applied Physics 26:766-775.

[6] Henrych J. The Dynamics of Explosion and Its Use, Developments in Atmospheric Science. Elsevier Scientific Publishing Company, Amsterdam, Netherlands, 1979.

[7] Kingery CN, Bulmash G (1984) Air blast parameters from TNT spherical air burst and hemispherical burst, Technical Report ARBRL-TR-02555:AD-B082 713, U.S. Army Ballistic Research Laboratory, Aberdeen Proving Ground, MD.

[8] Kinney GF, Graham, KJ. Explosive Shocks in Air. Springer Publishing Company, Berlin, Germany, 1985.

[9] Mills CA. The design of concrete structures to resist explosions and weapon effects. The first International Conference on Concrete for Hazard Protections, 27-30 September 1987, Edinburgh, UK.

[10] Sadovskiy MA (2004) Mechanical effects of air shock waves from explosions according to experiments, Selected works: Geophysics and Physics of Explosion, Nauka Press, Moscow.

[11] Luccioni BM, Ambrosini RD, Danesi RF (2004) Analysis of building collapse under blast loads. Engineering Structures 26(1):63-71.

[12] Jayasooriya R, Thambiratnam DP, Perera NJ, Kosse V (2011) Blast and residual capacity analysis of reinforced concrete framed buildings. Engineering Structures 33(12):3483-3495.

[13] Draganić H, Sigmund V (2012) Blast loading on structures. Technical Gazette 19(3):643-652.

[14] Kelliher D, Sutton-Swaby K (2012) Stochastic representation of blast load damage in a reinforced concrete building. Structural Safety 34(1):407-417.

[15] Yalciner H (2014) Structural response to blast loading: the effects of corrosion on reinforced concrete structures. Shock and Vibration 529892:1-7.

[16] Coffield A, Adeli H (2015) Irregular steel building structures subjected to blast loading. Journal of Civil Engineering and Management 22(1):17-25.

[17] Shi Y, Stewart MG (2015) Spatial reliability analysis of explosive blast load damage to reinforced concrete columns. Structural Safety 53:13-25.

[18] Syed ZI, Mohamed OA, Murad K, Kewalramani M (2017) Performance of earthquake-resistant rcc frame structures under blast explosions. Procedia Engineering 180:82-90.

[19] Tang EKC, Hao H (2010) Numerical simulation of a cable-stayed bridge response to blast loads, Part I: Model development and response calculations. Engineering Structures 32(10):3180-3192.

[20] Son J, Lee HJ (2011) Performance of cable-stayed bridge pylons subjected to blast loading. Engineering Structures 33(4):1133–1148.

[21] Andreou M, Kotsoglou A, Pantazopoulou S (2016) Modelling blast effects on a reinforced concrete bridge. Advances in Civil Engineering: 4167329:1–11.

[22] Hacıefendioğlu K (2017) Stochastic dynamic response of short-span highway bridges to spatial variation of blasting ground vibration. Applied Mathematics and Computation 292:194-209.

[23] Hashemi SK, Bradford MA, Valipour HR (2017) Dynamic response and performance of cable-stayed bridges under blast load: Effects of pylon geometry. Engineering Structures 137:50-66.

[24] Yusof MA, Rosdi RN, Nor NM, Ismail A, Yahya MA, Peng NC (2014) Simulation of reinforced concrete blast wall subjected to air blast loading. Journal of Asian Scientific Research 4(9):522-533.

[25] Hacıefendioğlu K, Koç V (2016) Dynamic assessment of partially damaged historic masonry bridges under blast-induced ground motion using multi-point shock spectrum method. Applied Mathematical Modelling 40 (23-24):10088-10104.

[26] Eamon CD, Baylot JT, O'Daniel JL (2004) Modeling concrete masonry walls subjected to explosive loads. Journal of Engineering Mechanics 130(9):1098–1106.

[27] Wu C, Hao H, Lu Y (2005) Dynamic response and damage analysis of masonry structures and masonry infilled RC frames to blast ground motion. Engineering Structures 27(3):323-333.

[28] Wu C, Hao H (2007) Safe scaled distance for masonry infilled RC frame structures subjected to air blast loads. Journal of Performance of Constructed Facilities 21(6):422–431.

[29] Wei X, Stewart MG (2010) Model validation and parametric study on the blast response of unreinforced brick masonry walls. International Journal of Impact Engineering 37(11):1150-1159.

[30] Davidson JS, Porter JR, Dinan RJ, Hammons MI, Connell JD (2004) Explosive testing of polymer retrofit masonry walls. Journal of Performance of Constructed Facilities 18(2):100-106.

[31] Baylot JT, Bullock B, Slawson TR, Woodson SC (2005) Blast response of lightly attached concrete masonry unit walls. Journal of Structural Engineering 131(8):1186-1193.

[32] Zapata BJ, Weggel DC (2008) Collapse study of an unreinforced masonry bearing wall building subjected to internal blast loading. Journal of Performance of Constructed Facilities 22(2):92-100.

[33] Chen L, Fang Q, Fan J, Zhang Y, Hao H, Liu J (2014) Responses of masonry infill walls retrofitted with CFRP, steel wire mesh and laminated bars to blast loadings. Advances in Structural Engineering 17(6):817-836.

[34] Alsayed SH, Elsanadedy HM, Al-Zaheri ZM, Al-Salloum YA, Abbas H (2016) Blast response of GFRP-strengthened infill masonry walls. Construction and Building Materials 115:438-451.

[35] Keys RA, Clubley SK (2017) Establishing a predictive method for blast induced masonry debris distribution using experimental and numerical methods. Engineering Failure Analysis 82:82-91.

[36] Gu M, Ling X, Wang H, Yu A, Chen G (2019) Experimental and numerical study of polymer-retrofitted masonry walls under gas explosions. Processes 7(12):863.

[37] ANSYS Workbench (2016) Swanson Analyses System, Ansys Inc, USA.

[38] ANSYS Autodyn (2016) Swanson Analyses System, Ansys Inc, USA.

[39] Ngo T, Mendis P, Gupta A, Ramsay J (2007) Blast loading and blast effects on structures-an overview. Electronic Journal of Structural Engineering 7:76-91.

[40] Smith PD, Hetherington JG. Blast and Ballistic Loading of Structures, 2nd edition, Boston, 1994.

[41] TBEC (2018) Turkish Building Earthquake Code, Disaster and Emergency Management Presidency, Ankara, Turkey.

[42] Riedel W, Thoma K, Hiermaier S, Schmolinske E. Penetration of reinforced concrete by BETA-B-500 numerical analysis using a new macroscopic concrete model for hydrocodes. The 9th

International Symposium on the Effects of Munitions with Structures, 03-07 May 1999, Berlin-Strausberg, Germany.

[43] Herrmann W (1969) Constitutive equation for the dynamic compaction of ductile porous materials. Journal of Applied Physics 40(6):2490-2499.

[44] UFC 3-340-02 (2008) Unified Facilities Criteria: Structures to resist the effects of accidental explosions, Department of Defense, Washington, USA.

[45] Sevim B, Toy AT (2019) Blasting response of a two-storey RC building under different charge weight of TNT explosives. Iranian Journal of Science and Technology, Transactions of Civil Engineering 44:565-577.

[46] Chiquito M, López LM, Castedo R, Pérez-Caldentey A, Santos AP (2019) Behaviour of retrofitted masonry walls subjected to blast loading: Damage assessment. Engineering Structures, 201,109805.

[47] Chen L, Fang Q, Jiang C, Fan J, Hao H (2013) Response and damage level of confined masonry walls to blast. Disaster Advances, 6(S4):380-394.